



Two Point Mutations in Old World Hantavirus Glycoproteins Afford the Generation of Highly Infectious Recombinant Vesicular Stomatitis Virus Vectors

 Megan M. Slough,^a  Kartik Chandran,^a  Rohit K. Jangra^a

^aDepartment of Microbiology and Immunology, Albert Einstein College of Medicine, Bronx, New York, USA

ABSTRACT Rodent-to-human transmission of hantaviruses is associated with severe disease. Currently, no FDA-approved, specific antivirals or vaccines are available, and the requirement for high biocontainment (biosafety level 3 [BSL-3]) laboratories limits hantavirus research. To study hantavirus entry in a BSL-2 laboratory, we set out to generate replication-competent, recombinant vesicular stomatitis viruses (rVSVs) bearing the Gn and Gc (Gn/Gc) entry glycoproteins. As previously reported, rVSVs bearing New World hantavirus Gn/Gc were readily rescued from cDNAs, but their counterparts bearing Gn/Gc from the Old World hantaviruses, Hantaan virus (HTNV) or Dobrava-Belgrade virus (DOBV), were refractory to rescue. However, serial passage of the rescued rVSV-HTNV Gn/Gc virus markedly increased its infectivity and capacity for cell-to-cell spread. This gain in viral fitness was associated with the acquisition of two point mutations: I532K in the cytoplasmic tail of Gn and S1094L in the membrane-proximal stem of Gc. Follow-up experiments with rVSVs and single-cycle VSV pseudotypes confirmed these results. Mechanistic studies revealed that both mutations were determinative and contributed to viral infectivity in a synergistic manner. Our findings indicate that the primary mode of action of these mutations is to relocalize HTNV Gn/Gc from the Golgi complex to the cell surface, thereby affording significantly enhanced Gn/Gc incorporation into budding VSV particles. Finally, I532K/S1094L mutations in DOBV Gn/Gc permitted the rescue of rVSV-DOBV Gn/Gc, demonstrating that incorporation of cognate mutations into other hantaviral Gn/Gc proteins could afford the generation of rVSVs that are otherwise challenging to rescue. The robust replication-competent rVSVs, bearing HTNV and DOBV Gn/Gc, reported herein may also have utility as vaccines.

IMPORTANCE Human hantavirus infections cause hantavirus pulmonary syndrome in the Americas and hemorrhagic fever with renal syndrome (HFRS) in Eurasia. No FDA-approved vaccines and therapeutics exist for these deadly viruses, and their development is limited by the requirement for high biocontainment. In this study, we identified and characterized key amino acid changes in the surface glycoproteins of HFRS-causing Hantaan virus that enhance their incorporation into recombinant vesicular stomatitis virus (rVSV) particles. The replication-competent rVSVs encoding Hantaan virus and Dobrava-Belgrade virus glycoproteins described in this work provide a powerful and facile system to study hantavirus entry under lower biocontainment and may have utility as hantavirus vaccines.

KEYWORDS Dobrava-Belgrade virus, Hantaan virus, hantavirus, recombinant vesicular stomatitis, viral entry, viral glycoproteins

Rodent-borne hantaviruses (family *Hantaviridae* of segmented negative-strand RNA viruses) cause hemorrhagic fever with renal syndrome (HFRS) in Eurasia and hantavirus pulmonary syndrome (HPS) in the Americas (1). Globally, more than 150,000

Citation Slough MM, Chandran K, Jangra RK. 2019. Two point mutations in Old World hantavirus glycoproteins afford the generation of highly infectious recombinant vesicular stomatitis virus vectors. *mBio* 10:e02372-18. <https://doi.org/10.1128/mBio.02372-18>.

Editor Anne Moscona, Columbia University Medical College

Copyright © 2019 Slough et al. This is an open-access article distributed under the terms of the [Creative Commons Attribution 4.0 International license](https://creativecommons.org/licenses/by/4.0/).

Address correspondence to Kartik Chandran, kartik.chandran@einstein.yu.edu, or Rohit K. Jangra, rohit.jangra@einstein.yu.edu.

Received 29 October 2018

Accepted 27 November 2018

Published 8 January 2019

cases of hantavirus disease occur per year. Human population growth, accelerating climate change, and habitat loss are predicted to increase the size and severity of hantavirus disease outbreaks (2–6). Although inactivated viral vaccines are in use in Asia for HFRS-causing Seoul (SEOV) and Hantaan (HTNV) viruses, their protective efficacy is moderate at best (7–9), and no FDA-approved hantavirus vaccines or antivirals are available. The development of hantavirus countermeasures is hampered by our limited understanding of the molecular mechanisms of viral replication and disease pathogenesis, the lack of tools available to investigate these mechanisms, and the need to perform hantavirus research under high biocontainment.

The development of surrogate viral systems (10, 11) that recapitulate cell entry and infection under biosafety level 2 (BSL-2) containment (or lower) has greatly accelerated both basic mechanistic investigations of virulent emerging viruses and the development of vaccines and therapeutics to target them (12–15). Several such systems have been described for hantaviruses, whose Gn and Gc glycoproteins (Gn/Gc) are necessary and sufficient for viral entry (16). When expressed in cells, with or without the nucleoprotein N, Gn/Gc were shown to self-assemble to produce virus-like particles (VLPs) with utility for studies of viral glycoprotein maturation and assembly (17–19) and as potential vaccine vectors (18). Single-cycle gammaretroviral and lentiviral vectors, bearing HTNV or Andes virus (ANDV) Gn/Gc, have been employed for viral entry and antibody neutralization studies and as candidate vectors for vaccination and gene therapy (20–24). Consistent with the flexibility of heterologous protein incorporation into the budding virions of vesicular stomatitis virus (VSV), multiple groups have also developed VSV-based single-cycle pseudovirions (pVSVs) for both HFRS-causing hantaviruses (HTNV [16, 25–27], Puumala virus [PUUV] [26, 28], and SEOV [16]) and HPS-causing hantaviruses (ANDV [29] and Sin Nombre virus [SNV] [27]).

Although single-cycle pseudovirions have advanced our understanding of hantavirus Gn/Gc assembly, viral entry, and antiviral immune responses, they are labor-intensive to generate in high yield. In contrast, self-replicating, recombinant VSVs (rVSVs), whose genomes have been modified to carry the hantavirus M gene (encoding Gn/Gc) in place of the VSV glycoprotein (G) gene, are relatively easy to produce in quantity, readily amenable to forward-genetic and small-molecule screens, and are unique among surrogate systems in affording forward-genetic selections to identify escape mutants against neutralizing antibodies and small-molecule entry inhibitors (30–33). Brown et al. (34) were the first to generate a rVSV bearing ANDV Gn/Gc and showed that it could protect Syrian hamsters against lethal ANDV challenge when administered as a vaccine (34, 35). Similar viruses have been used to identify host factors required for ANDV entry (27, 36). To expand the pool of such rVSVs for hantavirus research, we previously rescued a rVSV bearing SNV Gn/Gc from cDNA (36). However, rVSVs bearing Gn/Gc from the HFRS-causing Hantaan virus (HTNV) or Dobrava-Belgrade virus (DOBV) proved challenging to rescue.

Here, we show that serial passage of the initial rVSV-HTNV Gn/Gc stock in cell culture afforded the generation of a variant with enhanced replicative fitness suitable for viral entry studies. We mapped this gain in viral fitness to the acquisition of two point mutations: I532K in the cytoplasmic tail of Gn and S1094L in the stem region of Gc. Mechanistic studies revealed that these mutations enhance rVSV infectivity by relocalizing HTNV Gn/Gc from the Golgi complex to the cell surface, thereby augmenting Gn/Gc incorporation into budding VSV particles. Finally, incorporation of these two mutations into DOBV Gn/Gc afforded success in rVSV-DOBV Gn/Gc rescue. Our results suggest that selection- and protein engineering-based approaches to boost the cell surface expression of entry glycoproteins from other hantaviruses, or even more divergent bunyaviruses, could enable the generation of rVSVs that are otherwise refractory to rescue and replicate only poorly. The rVSV vectors described herein may have utility as vaccines.

RESULTS

Two point mutations in the Gn/Gc complex enhance the generation of infectious rVSV-HTNV Gn/Gc and pVSV-HTNV Gn/Gc. Hantaviruses causing human disease are classified as biosafety level 3 (BSL-3) agents by the CDC. To study hantavirus entry and infection in a BSL-2 setting, we attempted to generate a replication-competent, recombinant vesicular stomatitis virus (rVSV) expressing the Gn/Gc glycoproteins of Hantaan virus (HTNV) (strain 76-118), a prototypic HFRS-causing hantavirus. Multiplication and spread of the early passage rVSV bearing HTNV Gn/Gc were poor but improved dramatically following three serial passages in Vero cells. Analysis of the selected viral population identified two amino acid changes in Gn/Gc, one located in the cytoplasmic tail of Gn (I532K) and the other in the membrane-proximal stem of the Gc ectodomain (S1094L) (Fig. 1A). To determine whether either one or both of these two mutations could account for enhanced viral multiplication, we attempted to rescue rVSV-HTNV Gn/Gc viruses from cDNAs, incorporating each mutation separately and together. We successfully recovered both single and double mutant viruses, but not the rVSV bearing the parental strain 76-118 HTNV Gn/Gc (hereafter identified as “wild type”). Analyses of the viruses produced from Vero cells, infected with equivalent volumes of rescue supernatants from 293FT cells, revealed that the Gn/Gc double mutant virus (I532K/S1094L) multiplied and spread more rapidly than either single mutant virus (Fig. 1B and C).

To confirm the determinative role of each Gn/Gc mutation and exclude potentially confounding effects from mutations elsewhere in the viral genome, we generated and analyzed single-cycle VSV pseudotypes (pVSVs) bearing wild-type (WT) and mutant Gn/Gc proteins. Consistent with our findings with the rVSVs, pVSVs bearing the HTNV Gn/Gc (I532K/S1094L) double mutant displayed a higher specific (per-particle) infectivity in Vero cells than those bearing either single mutant or WT Gn/Gc (Fig. 1D), after normalization of each viral preparation for particle number (Fig. 1E). Further, the Gc mutant was more infectious than WT. Together, these findings indicate that the I532K and S1094 mutations in HTNV Gn and Gc, respectively, confer a synergistic enhancement in infectivity when present in the same viral particles.

The I532K/S1094L mutations do not enhance Gn/Gc expression. To uncover the mechanism by which the mutations I532K and S1094L enhance VSV-HTNV Gn/Gc infectivity, we first examined the effects of these mutations on Gn/Gc expression. We transfected 293T cells with plasmids encoding WT or mutant Gn/Gc and used a cell-based ELISA to determine the relative Gn/Gc levels (see Materials and Methods for details). Cells were permeabilized to render Gn/Gc in all subcellular compartments accessible to immunodetection by the conformation-sensitive, HTNV Gc-specific monoclonal antibody 3G1 (37). At 48 h posttransfection, the I532K/S1094L double mutation modestly elevated Gn/Gc expression in comparison to WT, although I532K had little or no effect, and S1094L modestly depressed Gn/Gc expression (Fig. 2). However, none of these changes were statistically significant. These findings suggest that an increase in the steady-state levels of Gn/Gc is not the primary mechanism by which the I532K/S1094L mutations enhance VSV-HTNV Gn/Gc infectivity.

The I532K/S1094L mutations together enhance localization of Gn/Gc at the plasma membrane. Both VSV and HTNV acquire their surface glycoproteins in the secretory pathway during viral budding; however, they do so in distinct cellular compartments. Specifically, VSV particles bud at the plasma membrane, whereas HTNV particles, like those of many hantaviruses and other bunyaviruses, are reported to bud into the Golgi apparatus. In keeping with these observations, VSV G and HTNV Gn/Gc (Fig. 3 and 4) localize primarily to the plasma membrane and endoplasmic reticulum (ER)/Golgi apparatus, respectively (38–40). We postulated that this mismatch in the subcellular sites of viral budding and glycoprotein localization may account for the poor growth of rVSV-HTNV Gn/Gc and that the I532K/S1094L mutations might ameliorate this mismatch. Accordingly, we examined the subcellular distribution of WT and mutant Gn and Gc proteins in transfected U2OS cells by immunofluorescence (IF) microscopy. Gn and Gc colocalization was essentially complete for all variants (Fig. 3),

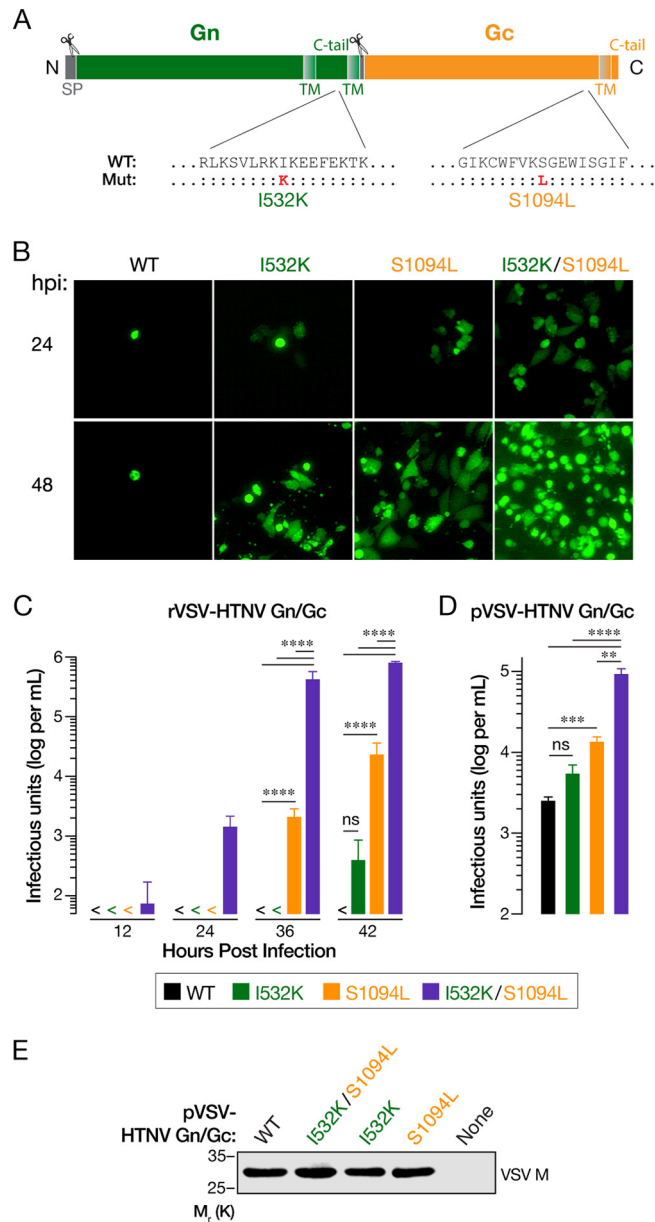


FIG 1 Two point mutations (I532K and S1094L) in the Gn/Gc enhance rVSV-HTNV Gn/Gc and pVSV-HTNV Gn/Gc infectivity. (A) Schematic representation of the HTNV Gn/Gc. Locations of the point mutations acquired after serial passaging of rVSV expressing HTNV Gn/Gc are shown. (B and C) Growth of WT or mutant rVSV-HTNV Gn/Gc. Supernatants from 293FT cells cotransfected with plasmids encoding rVSV genomes expressing eGFP bearing WT, I532K, S1094L, or I532K/S1094L versions of HTNV Gn/Gc with helper plasmids, were used to infect Vero cells. (B) Representative images of eGFP expression in Vero cells at the indicated times postinfection (hours postinfection [hpi]). (C) The titers of the virus in supernatants collected from infected Vero cells at indicated times postinfection were determined on naive Vero cells. Data from two independent experiments ($n = 4$) are represented as log infectious units (IU) per ml (mean plus standard deviation [SD] [error bar]). Virus titers that were below the limit of detection (50 IU per ml) (<) are indicated. Groups were compared by two-way ANOVA with Tukey's correction for multiple comparisons. ns, not significant ($P > 0.05$); ****, $P < 0.0001$. (D) Production of single-cycle VSV pseudotypes (pVSV). 293T cells expressing WT, I532K, S1094L, or I532K/S1094L forms of HTNV Gn/Gc in *trans* were infected with VSV-eGFP- Δ G (VSV expressing eGFP, carrying the VSV G glycoprotein on its surface, but lacking the G gene) 48 h later. Following extensive washing to remove VSV G-carrying residual viruses, supernatants were collected at 48 h postinfection, and infectious titers were measured on Vero cells. Means plus standard errors of the means (SEM) from four independent experiments ($n = 8$) are shown here. Background VSV pseudotype production from empty vector-transfected cells was below the limit of detection (100 IU per ml). Groups were compared by one-way ANOVA with Tukey's correction for multiple comparisons. ns, $P > 0.05$; **, $P < 0.01$; ***, $P < 0.001$; ****, $P < 0.0001$. (E) HTNV Gn/Gc mutations do not affect overall VSV particle production. Equivalent amounts (by volume) of pelleted VSV pseudotypes from panel D were analyzed by VSV M-specific immunoblotting. A representative blot from three independent experiments is shown.

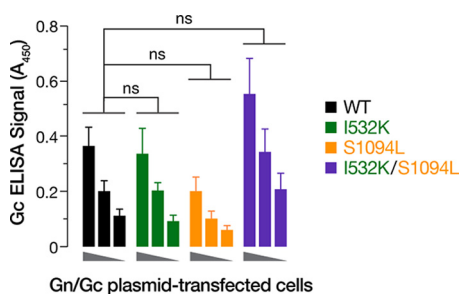


FIG 2 The HTNV Gn/Gc mutations do not enhance Gc production. 293T cells, transfected with plasmids expressing empty vector or WT, I532K, S1094L, or I532K/S1094L forms of HTNV Gn/Gc, were fixed at 48 h posttransfection. Following permeabilization, cells were tested for HTNV total Gc expression using an in-cell ELISA. To ensure linearity of the ELISA, serial twofold dilutions of the transfected cells were made by mixing them with untransfected cells. Data were graphed after background ELISA signal from empty vector-transfected 293T cells was subtracted. Data from three independent experiments ($n = 5$ or 6) are shown as mean \pm SEM. Groups were compared by one-way ANOVA with Tukey's correction for multiple comparisons. ns, $P > 0.05$.

showing that the mutations do not alter relative Gn and Gc distribution in cells. We further noted a predominantly perinuclear Gn/Gc staining for all variants that colocalized with GM130, a marker for the Golgi apparatus, but not with an ER marker, calreticulin (Fig. 4), indicating that the mutants substantially retain Golgi localization. Interestingly, however, some cells expressing the double mutant also displayed marked Gn/Gc staining in the cell periphery (yellow arrowheads in Fig. 3 and 4), suggesting that a subset of these molecules do localize to the plasma membrane.

To directly examine this possibility, we immunostained U2OS cells transfected with plasmids expressing WT or mutant Gn/Gc to visualize the cell surface expres-

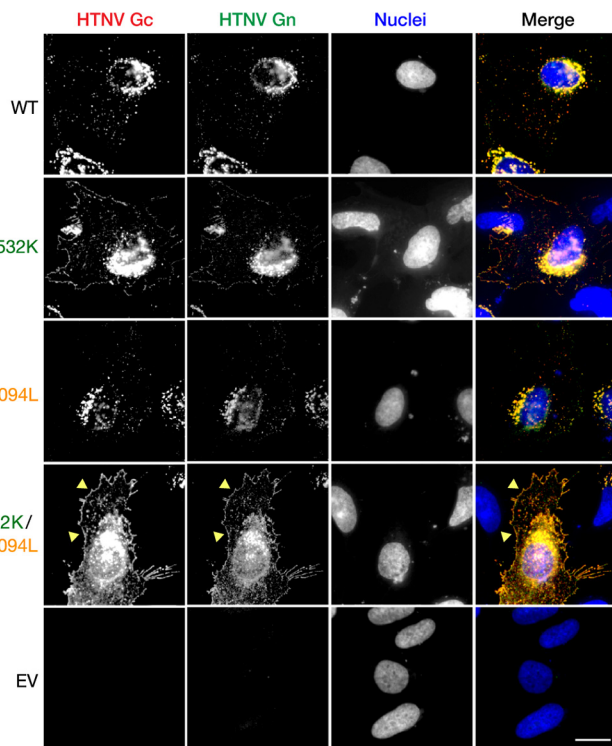


FIG 3 The HTNV Gn/Gc mutations do not alter glycoprotein colocalization. Human osteosarcoma U2OS cells, transfected with plasmids expressing WT, I532K, S1094L, or I532K/S1094L variants of HTNV Gn/Gc, were fixed at 24 h posttransfection, permeabilized, and coimmunostained with HTNV Gn- and Gc-specific antibodies (see Materials and Methods for details). EV, empty vector. Representative images from a single experiment, out of at least three experiments are shown. Bar, 20 μ m.

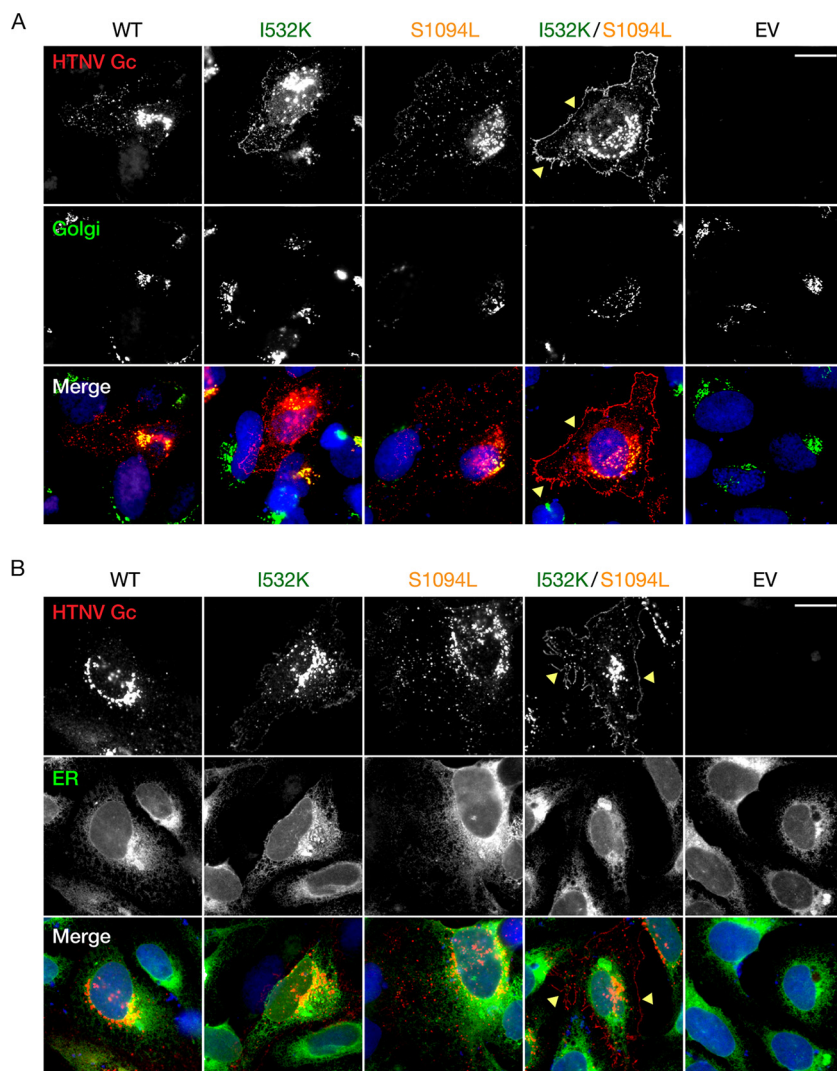


FIG 4 Trafficking of HTNV Gn/Gc to the Golgi apparatus is unaffected by I532K and S1094L mutations. (A) Human osteosarcoma U2OS cells, transfected with plasmids expressing WT, I532K, S1094L, or I532K/S1094L forms of HTNV Gn/Gc, were fixed at 24 h posttransfection, permeabilized, and costained with HTNV Gc-specific (3G1) and either Golgi apparatus-specific (GM130) antibody (A) or ER-specific (calreticulin) antibody (B). EV, empty vector. Representative images from a single experiment, out of at least two independent experiments, are shown. Bars, 20 μ m.

sion of these glycoproteins. The Gn mutation alone mildly enhanced the cell surface expression of both Gn and Gc, whereas the Gc mutation alone had little or no effect. Interestingly, the double mutant afforded an even higher level of cell surface Gn/Gc expression, indicating that the Gc mutation can act in concert with its Gn counterpart to drive relocalization of Gn/Gc to the plasma membrane (Fig. 5A). Similar results were obtained with primary human umbilical vein endothelial cells (HUVECs) transfected with HTNV Gn/Gc expression plasmids (Fig. 5B). Quantitation of cell surface Gc expression in plasmid-transfected U2OS cells by flow cytometry (Fig. 5C and D) and in 293T cells by on-cell ELISA (Fig. 5E), further corroborated the synergistic enhancement of Gn/Gc cell surface expression conferred by the I532K and S1094L mutations.

HTNV-Gn/Gc mutations collectively increase viral glycoprotein incorporation into VSV virions. Because VSV virions are known to acquire heterologous membrane proteins during viral budding at the host cell plasma membrane, we reasoned that enhanced cell surface expression of mutant HTNV Gn/Gc might increase

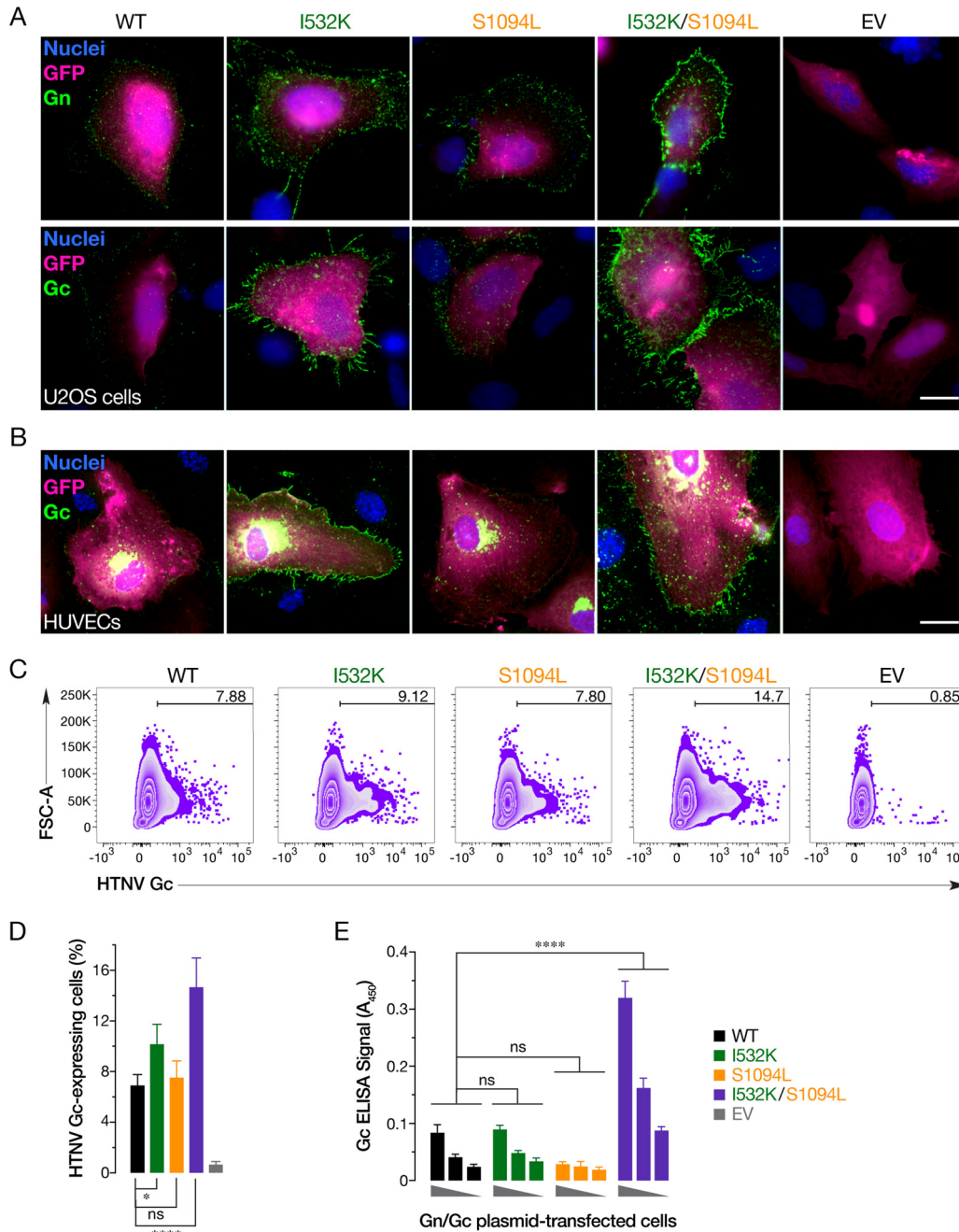


FIG 5 The HTNV Gn/Gc I532K and S1094L mutations together enhance plasma membrane localization of Gn/Gc. (A) U2OS cells, cotransfected with plasmids expressing eGFP and WT, I532K, S1094L, or I532K/S1094L forms of HTNV Gn/Gc, were stained for cell surface expression of HTNV Gn or Gc at 48 h posttransfection. (B) Primary human endothelial cells (HUVECs), nucleofected with plasmids encoding eGFP and WT, I532K, S1094L, or I532K/S1094L versions of HTNV Gn/Gc, were fixed 72 h later, permeabilized, and stained with HTNV Gc-specific antibody. Representative images from a single experiment, illustrating at least three independent experiments, are shown for each image in panels A and B. EV, empty vector. Bars, 20 μ m. (C and D) U2OS cells, transfected as described above for panel A, were immunostained for cell surface expression of HTNV Gc using an anti-HTNV Gc MAb 3G1 and analyzed using flow cytometry. Representative FACS zebra plots from one experiment are represented in panel C. Data from three independent experiments are shown as means \pm SD in panel D. Groups were compared by one-way ANOVA with Tukey's correction for multiple comparisons. ns, $P > 0.05$; *, $P < 0.05$; ****, $P < 0.0001$. (E) 293T cells, transfected with plasmids expressing variants of HTNV Gn/Gc, were stained, at 48 h posttransfection, for cell surface expression of HTNV Gc, and detected by on-cell ELISA using Gc-specific MAb 3G1 (mean \pm SEM, $n = 5$ or 6 from three independent experiments). The values for the groups were compared by two-way ANOVA with Tukey's correction for multiple comparisons. ns, $P > 0.05$; ****, $P < 0.0001$.

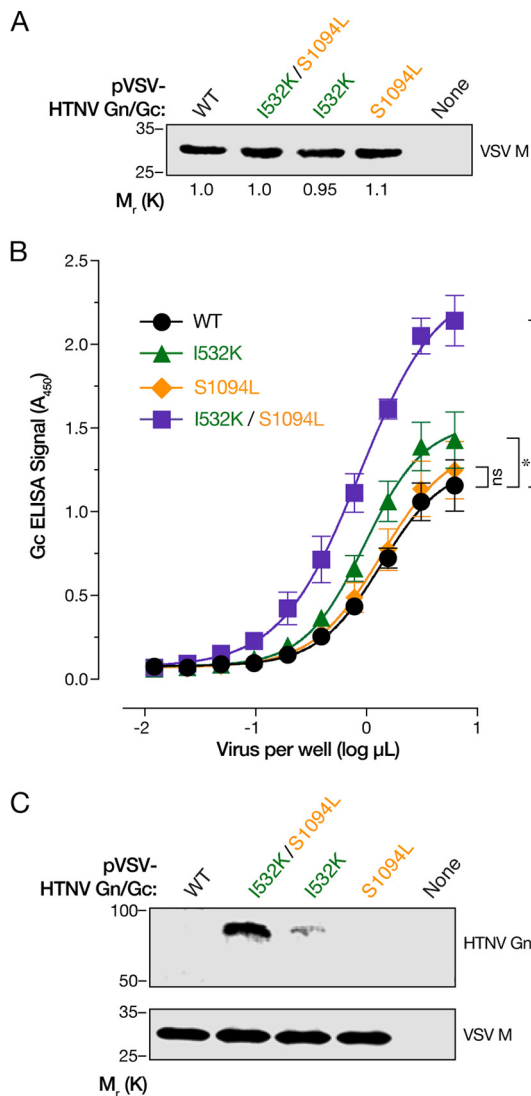


FIG 6 I532K and S1094L mutations collectively increase HTNV Gn/Gc incorporation into VSV virions. (A) Normalization of virus particles carrying HTNV Gn/Gc variants by immunoblotting for VSV matrix (M) protein. The numbers below the lanes in the blot indicate the relative amount of VSV M protein detected as compared to the WT. A blot representative of at least three independent experiments is shown here. (B) Serial twofold dilutions of normalized pVSV particles as ascertained in panel A, were captured on an ELISA plate and subjected to an HTNV Gc-specific ELISA (mean \pm SEM, $n = 8$ from four independent assays performed on two independent virus preparations). The values for groups were compared by two-way ANOVA with Tukey's correction for multiple comparisons. ns, $P > 0.05$; ****, $P < 0.0001$. (C) Immunoblots of HTNV Gn and VSV M proteins after normalization of pVSV particles. Representative blots from one out of two independent experiments are shown here.

incorporation of the latter into VSV particles. To test this hypothesis, we examined single-cycle VSV pseudotypes (pVSVs) bearing WT and mutant Gn/Gc proteins for HTNV Gn/Gc incorporation by HTNV Gc-specific ELISA and immunoblotting after normalizing viral particle content by VSV matrix protein M-specific immunoblotting (Fig. 6A and C). Concordant with their effects on the cell surface expression level of each glycoprotein, the Gn mutation alone enhanced incorporation of Gn/Gc into viral particles, whereas the Gc mutation did not, and combination of both mutations afforded a further synergistic increase in Gn/Gc incorporation (Fig. 6B and C). Taken together, these findings strongly suggest that relocalization of HTNV Gn/Gc from the Golgi complex to the plasma membrane, induced by the I532K/S1094L mutations, enhances rVSV-HTNV Gn/Gc infectivity by increasing viral glycoprotein incorporation into virus particles.

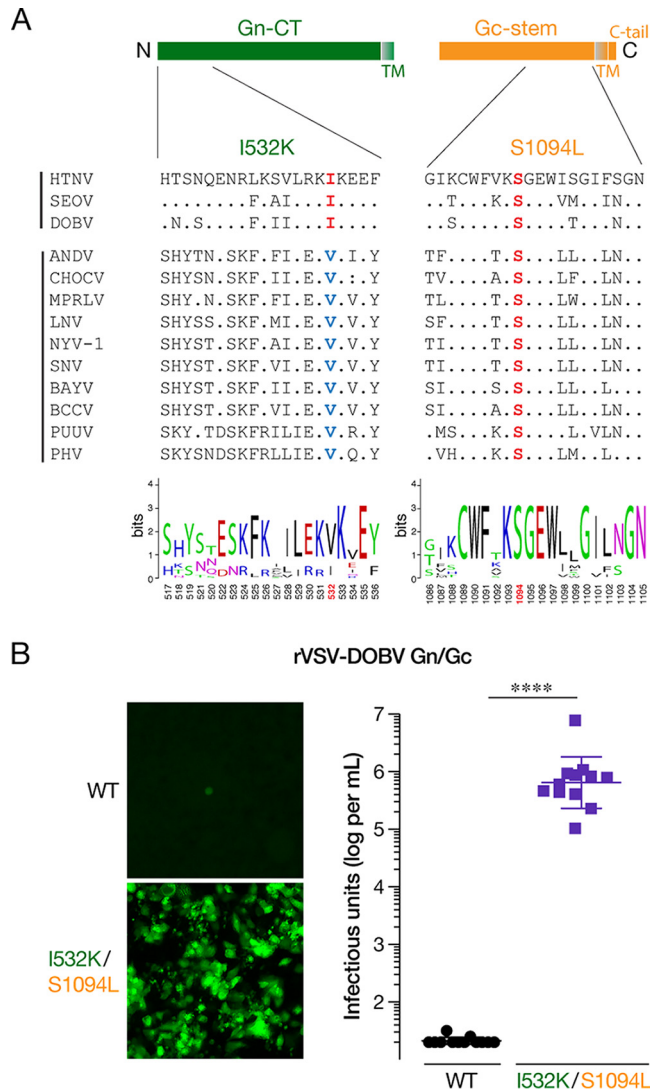


FIG 7 Incorporation of Gn/Gc mutations into the Old World DOBV glycoproteins affords the generation of rVSV-DOBV Gn/Gc. (A) Schematic of cytoplasmic tail of Gn and stem region of Gc is shown in the top panel. Alignment of amino acid sequences of the N-terminal 20 amino acids of the cytoplasmic tail of Gn and C-terminal 20 acids from 13 species of hantaviruses generated by Clustal Omega along with a WebLogo version (bottom panel) is shown. Abbreviations: HTNV, Hantaan virus; SEOV, Seoul virus; DOBV, Dobrava-Belgrade virus; ANDV, Andes virus; CHOVCV, Choclo virus; MPRLV, Maporal virus; LNV, Laguna Negra virus; NYV-1, New York-1 virus; SNV, Sin Nombre virus; BAYV, Bayou virus; BCCV, Black Creek Canal virus; PUUV, Puumala virus; PHV, Prospect Hill virus. (B) Supernatants from 293FT cells, cotransfected with plasmids encoding rVSV genomes expressing eGFP bearing WT or I532K/S1094L versions of DOBV Gn/Gc with helper plasmids, were used to infect Huh7.5.1 cells. (Left) Representative images of eGFP expression in Huh7.5.1 cells at 6 days postinfection. (Right) Titers of virus from supernatants collected from infected Huh7.5.1 cells 6 days postinfection were determined on naive Huh7.5.1 cells. Data from 12 independent rescues, from WT and I532K/S1094L versions of DOBV Gn/Gc, are represented as log infectious units (IU) per ml (mean \pm SD). The limit of detection is 20 IU per ml. Groups were compared by Mann Whitney U-test. ****, $P < 0.0001$.

Cognate mutations in another Old World hantavirus, DOBV, allow the successful generation of rVSV-DOBV Gn/Gc. Amino acid residues corresponding to I532 and S1094 in the Gn/Gc are conserved in HTNV, SEOV, and DOBV (Fig. 7A). To extend our findings to another hantavirus Gn/Gc, we incorporated the I532K and S1094L mutations into the DOBV Gn/Gc and set up rVSV rescue experiments in parallel with the parental WT version. The double mutant rVSV-DOBV Gn/Gc rescued every time (12 out of 12 independent rescues), while the WT did not (0 out of 12 independent rescues) (Fig. 7B and C), indicating that these mutations could be used to generate other rVSVs expressing hantavirus Gn/Gc that have previously been hard to generate.

DISCUSSION

Retroviral and vesiculoviral pseudotypes carrying heterologous viral glycoproteins have greatly enhanced our understanding of viral glycoprotein maturation and virus assembly (20, 21), helped delineate the roles of host factors in viral entry and other virus-host interactions (36, 41–43), assisted in deciphering mechanisms of immune response and correlates of protection (34, 44), and have successfully been used to isolate and characterize neutralizing antibodies (31, 45) and developed as vaccines (15, 34). Notwithstanding the remarkable ability of these virions to package heterologous glycoproteins that localize to the plasma membrane, not all viral entry glycoproteins are amenable to efficient pseudotyped virus production. Here, we combined the ability of rVSV to undergo mutations, akin to other RNA viruses, with forward genetic analyses to identify and characterize the roles of two point mutations, one each in the HTNV Gn (I532K) and Gc (S1094L), that greatly enhance infectivity. Moreover, we further corroborated and extended our findings by applying these mutations to generate an rVSV carrying another Old World hantavirus, DOBV Gn/Gc.

Like most members of the order *Bunyavirales*, HFRS-causing HTNV has been shown to bud at the Golgi cisternae (46, 47), with undetectable (48) or very low (16, 48, 49) amounts of Gn/Gc observed at the surfaces of cells expressing HTNV Gn/Gc. We hypothesized that I532K/S1094L mutations facilitate rVSV rescue by altering Gn/Gc expression and/or localization. Both of these mutations, alone or together, did not significantly affect total protein production (Fig. 2) or colocalization of Gn and Gc (Fig. 3). Although the majority of the single or double mutant Gn/Gc proteins were still localized to the Golgi complex (Fig. 4A), as were the WT proteins, the Gn mutation alone (I532K) or together with the Gc mutation (I532K/S1094L) showed significantly elevated cell surface expression as seen by immunofluorescence (Fig. 3, 4, and 5A and B), flow cytometry (Fig. 5C and D), and on-cell ELISA (Fig. 5E). As observed previously (16, 49), we also noted some WT HTNV Gn/Gc protein expression on the cell surface (Fig. 3 and 5). However, the I532K/S1094L mutations consistently enhanced cell surface expression, by three- to four-fold compared to the WT, in multiple human cell lines (U2OS and 293T), as well as primary cells (HUVECs), at multiple times posttransfection, suggesting that this phenotype is not limited to a particular cell type or time point (Fig. 3 and 5). Importantly, enriched cell surface expression correlated well with the levels of HTNV Gn/Gc incorporated in the vesiculoviral pseudovirions (Fig. 6), strongly indicating that relocation of Gn/Gc from the Golgi complex to the cell surface is one of the major mechanisms by which these mutations enhance rVSV-HTNV Gn/Gc infectivity. Moreover, the rVSV-HTNV Gn/Gc described here resembled the authentic HTNV (36) with respect to dependence on the sterol regulatory element-binding protein (SREBP) pathway and cholesterol requirements for entry and infection (27, 36), underscoring its utility for studying hantavirus entry. Although the topological locations of these mutations on Gn/Gc suggest that they are unlikely to have any effect on receptor usage and viral entry *per se*, more studies are required to formally address it.

Some bunyaviral glycoproteins, including those of hantaviruses, are expressed on the surfaces of virus-infected cells as well as glycoprotein cDNA-transfected cells (50–54). Consistent with the localization of readily detectable Gn/Gc on the surfaces of cells infected with HPS-causing viruses (53, 55), transmission electron microscopic studies show evidence of plasma membrane assembly of some New World hantaviruses such as SNV and Black Creek Canal virus (BCCV) (55, 56). Moreover, ANDV or SNV Gn and Gc can replace each other without affecting their normal trafficking (57). Interestingly, Gn of the HFRS-causing HTNV, DOBV, and SEOV carries an isoleucine at position 532 while that of the New World hantaviruses carries a valine (Fig. 7A). Congruent with these differences in cellular localization of their glycoproteins and virion budding sites, rescue of replication- and propagation-competent rVSVs carrying Gn/Gc from ANDV (34, 36) or SNV (36) was relatively easier than those carrying HTNV or DOBV Gn/Gc.

How does the I532K mutation enhance cell surface expression of HTNV Gn/Gc? I532 is located in the region that has been shown to bind hantavirus nucleoprotein and RNA

(58, 59), just upstream of the two zinc finger domains in the cytoplasmic tail of the Gn (Gn-CT) protein (Fig. 7A). Although Golgi retention of many bunyaviruses is mediated by Gn alone (60–65), signals in both hantavirus Gn and Gc seem to contribute to their Golgi localization. Gn proteins of HTNV (39), ANDV, or SNV (53, 57) are retained in the ER when expressed alone and need coexpression of Gc for their Golgi transport. In contrast, Pensiero and Hay (40) reported that HTNV Gn alone can localize to Golgi and the Golgi retention signal is likely located in the N-terminal 20 amino acids of the Gn-CT. The corresponding region of Gc from an orthobunyavirus Uukuniemi virus (UUKV), has also been suggested to be the Golgi retention signal for UUKV Gn/Gc (52). We hypothesize that the I532K mutation relocalizes HTNV Gn/Gc to the cell surface by disrupting its interaction with one or more unknown cellular factors that mediate Golgi retention. The rVSV system described here could be useful for further studies required to characterize this Golgi retention mechanism.

How the Gc (S1094L) mutation increases rVSV-HTNV Gn/Gc infectivity is less clear. It failed to enhance cell surface expression (Fig. 3 and 5) and VSV incorporation of Gn/Gc on its own (Fig. 6). This suggests that S1094L contributes to rVSV rescue via a mechanism that is distinct from Gn/Gc relocalization to the cell surface. S1094 is highly conserved across hantaviruses and is located in the membrane-proximal, C-terminal half of the Gc stem (Fig. 7A). The Gc stem is critical for the formation of the postfusion hairpin conformation (66), and peptides corresponding to its C-terminal half inhibit ANDV infection and membrane fusion (67). Most of the Gc stem, including the S1094 residue, was not visualized in the hantavirus Gc crystal structure (68, 69). Alteration in the physical curvature of the membrane by the membrane-proximal region of the VSV glycoprotein stem region has been proposed to enhance VSV budding efficiency (70). However, S1094L alone did not affect budding efficiency (Fig. 1E). We speculate that this mutation might alter intersubunit interactions and/or the glycoprotein fusogenicity. Further studies are required to understand the other mechanism(s) by which the Gc mutation facilitates the generation of rVSVs.

Together, our results suggest that the enhancement of cell surface expression of other bunyaviral glycoprotein(s) through incorporation of cognate mutations may enhance the utility of existing single-cycle VSV vectors bearing Old World hantavirus glycoproteins and facilitate the generation of rVSVs bearing these or other bunyaviral glycoproteins. Moreover, the enhancements in incorporation of Gn/Gc into pseudotyped virus particles and localization at the cell surface in infected cells might elicit a more immunogenic response and pave the way for novel VSV-based bunyaviral vaccines.

MATERIALS AND METHODS

Cells. Human osteosarcoma U2OS and embryonic kidney fibroblast 293T cells obtained from ATCC were cultured in modified McCoy's 5A medium (Thermo Fisher) and high-glucose Dulbecco's modified Eagle medium (DMEM) (Thermo Fisher) supplemented with 10% fetal bovine serum (FBS) (Atlanta Biologicals), 1% GlutaMAX (Thermo Fisher), and 1% penicillin-streptomycin (Pen-Strep; Thermo Fisher), respectively. The grivet kidney Vero cells (from ATCC) were cultured in DMEM supplemented with 2% FBS, 1% GlutaMAX, and 1% Pen-Strep. Human umbilical vein endothelial cells (HUVECs) (Lonza) were cultured in EGM medium supplemented with EGM-SingleQuots (Lonza). Huh-7.5.1 cells were cultured as described above for 293T cells, with the addition of 1% nonessential amino acids. All adherent cell lines were maintained in a humidified 37°C, 5% CO₂ incubator. Freestyle-293-F suspension-adapted HEK-293 cells (Thermo Fisher) were maintained in GIBCO FreeStyle 293 expression medium (Thermo Fisher) using shaker flasks at 115 rpm, 37°C, and 8% CO₂.

Plasmids. Plasmids encoding human codon-optimized Hantaan virus (HTNV) Gn and Gc glycoproteins (Gn/Gc) (76-118 strain, GenBank accession number [NP_941978.1](#)) and Dobrava-Belgrade virus (DOBV) Gn/Gc (Ano-Poroia/AF19 strain, GenBank accession number [NP_942554.1](#)) in the genome of vesicular stomatitis virus (VSV), carrying an eGFP gene, were generated as described previously (36). HTNV Gn/Gc point mutations (I532K, S1094L, or I532K/S1094L) and DOBV Gn/Gc mutations (I532K/S1094L) were cloned into the genomic VSV (described above) and pCAGGS plasmids using standard molecular biology techniques. Human codon-optimized variable heavy (VH) (GenBank accession number [FJ751231](#)) and light (VL) (GenBank accession number [FJ751232](#)) chain sequences of HTNV Gc-specific MAbs, 3G1 (37), were synthesized by Epoch Biosciences and cloned into the pMAZ heavy (IgH) and light (IgL) chain vectors (71), respectively. The sequences of all plasmid inserts were confirmed by Sanger sequencing.

Generation of recombinant and pseudotyped VSVs. Replication-competent, recombinant VSVs (rVSVs) bearing WT or Gn/Gc-mutant HTNV or DOBV Gn/Gc were generated using a plasmid-based rescue system in 293T cells as described previously (36, 72). When required, rescued viruses were propagated on either Vero (HTNV) or Huh7.5.1 (DOBV) cells, and HTNV and DOBV Gn/Gc sequences were amplified from viral genomic RNA by RT-PCR and analyzed by Sanger sequencing. Single-cycle VSVΔG pseudotypes, encoding an eGFP reporter, were produced in 293T cells as described previously (36, 72). Viral infection was scored by manually enumerating eGFP-expressing cells using an Axio Observer inverted microscope (Zeiss), as described previously (36) or using automated counting with Cytation-5 (Biotek).

Production of HTNV Gc-specific MAb 3G1. MAb 3G1 was purified from the supernatants of Freestyle-293-F suspension cells transiently cotransfected with pMAZ vectors expressing heavy and light chains of 3G1 as described previously (31).

Detection of HTNV Gn/Gc surface expression by flow cytometry. Human U2OS osteosarcoma cells, seeded in six-well plates 18 to 22 h prior to transfection, were transfected with 2 μ g of the pCAGGS vectors, expressing nothing or variants of HTNV Gn/Gc, and 0.5 μ g of a plasmid expressing eGFP. At 24 h posttransfection, cell plates were chilled on ice for 10 min and blocked with chilled 10% fetal bovine serum (FBS) in phosphate-buffered saline (PBS) for 30 min at 4°C. Surface HTNV Gc was stained using human anti-HTNV Gc MAb 3G1 (7 μ g/ml) followed by anti-human Alexa Fluor 555 (5 μ g/ml; Thermo Fisher) for 1 h at 4°C each. After extensive washing, cells were stained with Live/Dead Fixable Violet Dead Cell Stain kit (Invitrogen), washed again with PBS, and resuspended in PBS containing 2% FBS. Stained cells were passed through a 41- μ m nylon net filter (Millipore) and analyzed using a LSRII flow cytometer and FlowJo V.10 software. Representative FACS “zebra” plots were generated using the FlowJo V.10 software.

Immunofluorescence microscopy for HTNV Gn/Gc localization. Human U2OS osteosarcoma cells plated on fibronectin-coated glass coverslips were transfected with 500 ng of empty vector or HTNV Gn/Gc expression vectors together with 50 ng of eGFP-expressing plasmid as described above. At 24 h posttransfection, cells were fixed with 4% formaldehyde (Sigma) for 5 min and permeabilized with 0.1% Triton X-100 for 10 min at room temperature. After blocking, HTNV Gn and Gc were detected by incubating cells with an anti-HTNV Gn mouse MAb 3D5 (1:500 dilution; BEI Resources) followed by anti-mouse Alexa Fluor 488 antibody, or an anti-HTNV Gc human MAb 3G1 (5 μ g/ml) followed by anti-human Alexa Fluor 555 antibody (Thermo Fisher), respectively. Anti-GM130 (1 μ g/ml; BD Biosciences) was used to costain the Golgi apparatus, and anticalreticulin (1:400 dilution; Thermo Fisher) was used to costain the ER. For surface staining, cells were placed on ice 10 min prior to blocking for 30 min at 4°C and incubated with the above-described HTNV Gn or Gc antibodies on ice before fixing and staining with the secondary antibodies as described above. Primary human umbilical vein endothelial cells (HUVECs) were nucleofected with 5 μ g of empty vector or HTNV Gn/Gc-expressing vectors, together with 50 ng of an eGFP-expressing plasmid, using the Amaxa kit (program A-034; Lonza) before staining for total Gn/Gc expression at 72 h postnucleofection as described above for U2OS cells. Coverslips were mounted on slides with Prolong containing DAPI (Thermo Fisher) and were imaged using a Zeiss Axio Observer inverted microscope with a 40 \times objective.

In-cell ELISA for HTNV Gn/Gc expression. 293T cells, transfected with empty vector or vectors expressing various HTNV Gn/Gc variants using Lipofectamine 3000 (Invitrogen), were fixed with 4% formaldehyde (Sigma) for 5 min, and permeabilized with 0.1% Triton X-100 for 15 min at room temperature. After blocking with 5% FBS in PBS (1 h at room temperature), total HTNV Gn/Gc expression was detected by incubation with anti-HTNV Gc MAb 3G1 (0.7 μ g/ml, 1 h at room temperature) followed by anti-human HRP (Thermo Fisher) (1 h at room temperature). ELISA signal was developed using 1-Step Ultra TMB-ELISA substrate solution (Thermo Scientific) and measured on a Perkin Elmer Wallac 1420 Victor2 microplate reader. For measuring cell surface expression of HTNV Gn/Gc, live cells preblocked with 5% FBS in PBS (1 h on ice) were incubated with anti-HTNV Gc MAb 3G1 (0.7 μ g/ml, 1 h on ice) before fixing and incubation with the second antibody. No permeabilization step was involved. Absorbance values at 450 nm were corrected for background by subtracting the signal from cells transfected with an empty vector.

ELISA and immunoblots for HTNV Gn/Gc incorporation in VSV particles. To measure HTNV Gn/Gc incorporation into virus particles, we first normalized the ELISA input of single-cycle, pseudotyped vesicular stomatitis viruses (pVSVs) bearing HTNV Gn/Gc variants by immunoblotting (using mouse anti-VSV M MAb 23H12) for the VSV M content. Next, ELISA plates were coated with serial twofold dilutions of normalized pVSV particles bearing WT or Gn/Gc mutant HTNV glycoproteins overnight at 4°C. After blocking, HTNV Gc was detected using anti-HTNV Gc MAb 3G1 (0.7 μ g/ml) followed by anti-human HRP antibody (Thermo Fisher) by incubating for 1 h each at 37°C. ELISA was developed, and absorbance at 450 nm was measured as described above. For immunoblotting HTNV Gn, pVSV particles bearing HTNV Gn/Gc variants were normalized as described above, and Gn was detected using anti-HTNV Gn MAb 1F5/G2 (1:5,000 dilution; Austral Biologicals) and imaged with a LI-COR Odyssey Fc imager.

Hantavirus Gn/Gc sequence alignment. Alignment of amino acid sequences of the N-terminal 20 amino acids of the cytoplasmic tail of Gn and C-terminal 20 acids from 13 species of hantaviruses generated by Clustal Omega. The hantavirus sequences used for the alignment, along with their GenBank accession numbers, were as follows: Hantaan virus (HTNV), [NP_941978.1](#); Seoul virus (SEOV), [M34882.1](#); Dobrava-Belgrade virus (DOBV), [NP_942554.1](#); Andes virus (ANDV), [NP_604472.1](#); Choclo virus (CHOCV), [KT983772.1](#); Maporal virus (MPRLV), [NC_034552.1](#); Laguna Negra virus (LNV), [AF005728.1](#); New York-1 virus (NYV-1), [U36802.1](#); Sin Nombre virus (SNV), [NP_941974.1](#); Bayou virus (BAYV), [GQ244521.1](#); Black Creek Canal virus (BCCV), [L39950.1](#); Puumala virus (PUUV), [KT885051.1](#); Prospect Hill virus (PHV), [CAA38922.1](#). WebLogos were generated as described earlier (73).

ACKNOWLEDGMENTS

We thank Tyler Krause, Cecelia Harold, Tanwee Alkutkar, and Isabel Gutierrez for technical support and lab management. We would also like to acknowledge the Einstein Flow Cytometry Core for the use of their facility. The anti-Hantaan virus Gn-specific monoclonal antibody was obtained from the Joel M. Dalrymple – Clarence J. Peters USAMRIID Antibody Collection through BEI Resources, NIAID, NIH (monoclonal anti-Hantaan virus Gn glycoprotein, clone 3D5 [produced *in vitro*], NR-36162).

This work is supported by NIH grant AI132633 (to K.C.). K.C. was additionally supported by an Irma T. Hirsch/Monique Weill-Caulier Research Award. M.M.S. was additionally supported by NIH T32 training grant AI070117. The Einstein Flow Cytometry Core is supported by NCI center grant P30CA013330.

REFERENCES

- Jonsson CB, Figueiredo LTM, Vapalahti O. 2010. A global perspective on hantavirus ecology, epidemiology, and disease. *Clin Microbiol Rev* 23: 412–441. <https://doi.org/10.1128/CMR.00062-09>.
- Clement J, Vercauteren J, Verstraeten WW, Ducoffre G, Barrios JM, Vandamme A-M, Maes P, Van Ranst M. 2009. Relating increasing hantavirus incidences to the changing climate: the mast connection. *Int J Health Geogr* 8:1. <https://doi.org/10.1186/1476-072X-8-1>.
- Dearing MD, Dizney L. 2010. Ecology of hantavirus in a changing world. *Ann N Y Acad Sci* 1195:99–112. <https://doi.org/10.1111/j.1749-6632.2010.05452.x>.
- Holmes EC, Zhang Y-Z. 2015. The evolution and emergence of hantaviruses. *Curr Opin Virol* 10:27–33. <https://doi.org/10.1016/j.coviro.2014.12.007>.
- Yanagihara R, Gu SH, Arai S, Kang HJ, Song J-W. 2014. Hantaviruses: rediscovery and new beginnings. *Virus Res* 187:6–14. <https://doi.org/10.1016/j.virusres.2013.12.038>.
- Wu X, Lu Y, Zhou S, Chen L, Xu B. 2016. Impact of climate change on human infectious diseases: empirical evidence and human adaptation. *Environ Int* 86:14–23. <https://doi.org/10.1016/j.envint.2015.09.007>.
- Schmaljohn C. 2009. Vaccines for hantaviruses. *Vaccine* 27(Suppl 4): D61–D64. <https://doi.org/10.1016/j.vaccine.2009.07.096>.
- Maes P, Clement J, Van Ranst M. 2009. Recent approaches in hantavirus vaccine development. *Expert Rev Vaccines* 8:67–76. <https://doi.org/10.1586/14760584.8.1.67>.
- Jung J, Ko S-J, Oh HS, Moon SM, Song J-W, Huh K. 2018. Protective effectiveness of inactivated hantavirus vaccine against hemorrhagic fever with renal syndrome. *J Infect Dis* 217:1417–1420. <https://doi.org/10.1093/infdis/jiy037>.
- Schnell MJ, Buonocore L, Kretzschmar E, Johnson E, Rose JK. 1996. Foreign glycoproteins expressed from recombinant vesicular stomatitis viruses are incorporated efficiently into virus particles. *Proc Natl Acad Sci U S A* 93:11359–11365. <https://doi.org/10.1073/pnas.93.21.11359>.
- Soneoka Y, Cannon PM, Ramsdale EE, Griffiths JC, Romano G, Kingsman SM, Kingsman AJ. 1995. A transient three-plasmid expression system for the production of high titer retroviral vectors. *Nucleic Acids Res* 23: 628–633. <https://doi.org/10.1093/nar/23.4.628>.
- Takada A, Robison C, Goto H, Sanchez A, Murti KG, Whitt MA, Kawaoka Y. 1997. A system for functional analysis of Ebola virus glycoprotein. *Proc Natl Acad Sci U S A* 94:14764–14769. <https://doi.org/10.1073/pnas.94.26.14764>.
- Larson RA, Dai D, Hosack VT, Tan Y, Bolken TC, Hruba DE, Amberg SM. 2008. Identification of a broad-spectrum arenavirus entry inhibitor. *J Virol* 82:10768–10775. <https://doi.org/10.1128/JVI.00941-08>.
- Garbutt M, Liebscher R, Wahl-Jensen V, Jones S, Möller P, Wagner R, Volchkov V, Klenk H-D, Feldmann H, Ströher U. 2004. Properties of replication-competent vesicular stomatitis virus vectors expressing glycoproteins of filoviruses and arenaviruses. *J Virol* 78:5458–5465. <https://doi.org/10.1128/JVI.78.10.5458-5465.2004>.
- Regules JA, Beigel JH, Paolino KM, Voell J, Castellano AR, Hu Z, Muñoz P, Moon JE, Ruck RC, Bennett JW, Twomey PS, Gutiérrez RL, Remick SA, Hack HR, Wisniewski ML, Josleyn MD, Kwilas SA, Van Deusen N, Mbaya OT, Zhou Y, Stanley DA, Jing W, Smith KS, Shi M, Ledgerwood JE, Graham BS, Sullivan NJ, Jagodzinski LL, Peel SA, Alimonti JB, Hooper JW, Silvera PM, Martin BK, Monath TP, Ramsey WJ, Link CJ, Lane HC, Michael NL, Davey RT, Thomas SJ, rVSVΔG-ZEBOV-GP Study Group. 2017. A recombinant vesicular stomatitis virus ebola vaccine. *N Engl J Med* 376: 330–341. <https://doi.org/10.1056/NEJMoa1414216>.
- Ogino M, Ebihara H, Lee BH, Araki K, Lundkvist A, Kawaoka Y, Yoshimatsu K, Arikawa J. 2003. Use of vesicular stomatitis virus pseudotypes bearing hantaan or seoul virus envelope proteins in a rapid and safe neutralization test. *Clin Diagn Lab Immunol* 10:154–160. <https://doi.org/10.1128/CDLI.10.1.154-160.2003>.
- Betenbaugh M, Yu M, Kuehl K, White J, Pennock D, Spik K, Schmaljohn C. 1995. Nucleocapsid- and virus-like particles assemble in cells infected with recombinant baculoviruses or vaccinia viruses expressing the M and the S segments of Hantaan virus. *Virus Res* 38:111–124. [https://doi.org/10.1016/0168-1702\(95\)00053-5](https://doi.org/10.1016/0168-1702(95)00053-5).
- Li C, Liu F, Liang M, Zhang Q, Wang X, Wang T, Li J, Li D. 2010. Hantavirus-like particles generated in CHO cells induce specific immune responses in C57BL/6 mice. *Vaccine* 28:4294–4300. <https://doi.org/10.1016/j.vaccine.2010.04.025>.
- Acuña R, Cifuentes-Muñoz N, Márquez CL, Bulling M, Klingström J, Mancini R, Lozach P-Y, Tischler ND. 2014. Hantavirus Gn and Gc glycoproteins self-assemble into virus-like particles. *J Virol* 88:2344–2348. <https://doi.org/10.1128/JVI.03118-13>.
- Ma M, Kersten DB, Kamrud KI, Wool-Lewis RJ, Schmaljohn C, González-Scarano F. 1999. Murine leukemia virus pseudotypes of La Crosse and Hantaan Bunyaviruses: a system for analysis of cell tropism. *Virus Res* 64:23–32. [https://doi.org/10.1016/S0168-1702\(99\)00070-2](https://doi.org/10.1016/S0168-1702(99)00070-2).
- Cifuentes-Muñoz N, Darlix J-L, Tischler ND. 2010. Development of a lentiviral vector system to study the role of the Andes virus glycoproteins. *Virus Res* 153:29–35. <https://doi.org/10.1016/j.virusres.2010.07.001>.
- Cifuentes-Muñoz N, Barriga GP, Valenzuela PDT, Tischler ND. 2011. Aromatic and polar residues spanning the candidate fusion peptide of the Andes virus Gc protein are essential for membrane fusion and infection. *J Gen Virol* 92:552–563. <https://doi.org/10.1099/vir.0.027235-0>.
- Yu L, Bai W, Wu X, Zhang L, Zhang L, Li P, Wang F, Liu Z, Zhang F, Xu Z. 2013. A recombinant pseudotyped lentivirus expressing the envelope glycoprotein of hantaan virus induced protective immunity in mice. *Virol J* 10:301. <https://doi.org/10.1186/1743-422X-10-301>.
- Qian Z, Haessler M, Lemos JA, Arsenault JR, Aguirre JE, Gilbert JR, Bowler RP, Park F. 2006. Targeting vascular injury using Hantavirus-pseudotyped lentiviral vectors. *Mol Ther* 13:694–704. <https://doi.org/10.1016/j.ymthe.2005.11.016>.
- Lee B-H, Yoshimatsu K, Araki K, Okumura M, Nakamura I, Arikawa J. 2006. A pseudotype vesicular stomatitis virus containing Hantaan virus envelope glycoproteins G1 and G2 as an alternative to hantavirus vaccine in mice. *Vaccine* 24:2928–2934. <https://doi.org/10.1016/j.vaccine.2005.12.040>.
- Higa MM, Petersen J, Hooper J, Doms RW. 2012. Efficient production of Hantaan and Puumala pseudovirions for viral tropism and neutralization studies. *Virology* 423:134–142. <https://doi.org/10.1016/j.virol.2011.08.012>.
- Petersen J, Drake MJ, Bruce EA, Riblett AM, Didigu CA, Wilen CB, Malani N, Male F, Lee F-H, Bushman FD, Cherry S, Doms RW, Bates P, Briley K. 2014. The major cellular sterol regulatory pathway is required for Andes virus infection. *PLoS Pathog* 10:e1003911. <https://doi.org/10.1371/journal.ppat.1003911>.
- Paneth Iheozor-Ejiofor R, Levanov L, Hepojoki J, Strandin T, Lundkvist Å,

- Plyusnin A, Vapalahti O. 2016. Vaccinia virus-free rescue of fluorescent replication-defective vesicular stomatitis virus and pseudotyping with Puumala virus glycoproteins for use in neutralization tests. *J Gen Virol* 97:1052–1059. <https://doi.org/10.1099/jgv.0.000437>.
29. Ray N, Whidby J, Stewart S, Hooper JW, Bertolotti-Ciarlet A. 2010. Study of Andes virus entry and neutralization using a pseudovirion system. *J Virol Methods* 163:416–423. <https://doi.org/10.1016/j.jviromet.2009.11.004>.
 30. Wong AC, Sandesara RG, Mulherkar N, Whelan SP, Chandran K. 2010. A forward genetic strategy reveals destabilizing mutations in the Ebolavirus glycoprotein that alter its protease dependence during cell entry. *J Virol* 84:163–175. <https://doi.org/10.1128/JVI.01832-09>.
 31. Wec AZ, Herbert AS, Murin CD, Nyakatura EK, Abelson DM, Fels JM, He S, James RM, de La Vega M-A, Zhu W, Bakken RR, Goodwin E, Turner HL, Jangra RK, Zeitlin L, Qiu X, Lai JR, Walker LM, Ward AB, Dye JM, Chandran K, Bornholdt ZA. 2017. Antibodies from a human survivor define sites of vulnerability for broad protection against ebolaviruses. *Cell* 169: 878–890.e15. <https://doi.org/10.1016/j.cell.2017.04.037>.
 32. Kajihara M, Nakayama E, Marzi A, Igarashi M, Feldmann H, Takada A. 2013. Novel mutations in Marburg virus glycoprotein associated with viral evasion from antibody mediated immune pressure. *J Gen Virol* 94:876–883. <https://doi.org/10.1099/vir.0.049114-0>.
 33. Furuyama W, Marzi A, Nanbo A, Haddock E, Maruyama J, Miyamoto H, Igarashi M, Yoshida R, Noyori O, Feldmann H, Takada A. 2016. Discovery of an antibody for pan-ebolavirus therapy. *Sci Rep* 6:20514. <https://doi.org/10.1038/srep20514>.
 34. Brown KS, Safronetz D, Marzi A, Ebihara H, Feldmann H. 2011. Vesicular stomatitis virus-based vaccine protects hamsters against lethal challenge with Andes virus. *J Virol* 85:12781–12791. <https://doi.org/10.1128/JVI.00794-11>.
 35. Prescott J, DeBuyscher BL, Brown KS, Feldmann H. 2014. Long-term single-dose efficacy of a vesicular stomatitis virus-based Andes virus vaccine in Syrian hamsters. *Viruses* 6:516–523. <https://doi.org/10.3390/v6020516>.
 36. Kleinfelter LM, Jangra RK, Jae LT, Herbert AS, Mittler E, Stiles KM, Wirchnianski AS, Kielian M, Brummelkamp TR, Dye JM, Chandran K. 2015. Haploid genetic screen reveals a profound and direct dependence on cholesterol for hantavirus membrane fusion. *mBio* 6:e00801. <https://doi.org/10.1128/mBio.00801-15>.
 37. Yang J, Chen R, Wei J, Zhang F, Zhang Y, Jia L, Yan Y, Luo W, Cao Y, Yao L, Sun J, Xu Z, Yang A. 2010. Production and characterization of a recombinant single-chain antibody against Hantaan virus envelop glycoprotein. *Appl Microbiol Biotechnol* 86:1067–1075. <https://doi.org/10.1007/s00253-009-2379-8>.
 38. Brown EL, Lyles DS. 2003. Organization of the vesicular stomatitis virus glycoprotein into membrane microdomains occurs independently of intracellular viral components. *J Virol* 77:3985–3992. <https://doi.org/10.1128/JVI.77.7.3985-3992.2003>.
 39. Ruusala A, Persson R, Schmaljohn CS, Pettersson RF. 1992. Coexpression of the membrane glycoproteins G1 and G2 of Hantaan virus is required for targeting to the Golgi complex. *Virology* 186:53–64. [https://doi.org/10.1016/0042-6822\(92\)90060-3](https://doi.org/10.1016/0042-6822(92)90060-3).
 40. Pensiero MN, Hay J. 1992. The Hantaan virus M-segment glycoproteins G1 and G2 can be expressed independently. *J Virol* 66:1907–1914.
 41. Chandran K, Sullivan NJ, Felbor U, Whelan SP, Cunningham JM. 2005. Endosomal proteolysis of the Ebola virus glycoprotein is necessary for infection. *Science* 308:1643–1645. <https://doi.org/10.1126/science.1110656>.
 42. Carette JE, Raaben M, Wong AC, Herbert AS, Obernosterer G, Mulherkar N, Kuehne AI, Kranzusch PJ, Griffin AM, Ruthel G, Dal Cin P, Dye JM, Whelan SP, Chandran K, Brummelkamp TR. 2011. Ebola virus entry requires the cholesterol transporter Niemann-Pick C1. *Nature* 477: 340–343. <https://doi.org/10.1038/nature10348>.
 43. Jae LT, Raaben M, Herbert AS, Kuehne AI, Wirchnianski AS, Soh TK, Stubbs SH, Janssen H, Damme M, Saftig P, Whelan SP, Dye JM, Brummelkamp TR. 2014. Lassa virus entry requires a trigger-induced receptor switch. *Science* 344:1506–1510. <https://doi.org/10.1126/science.1252480>.
 44. Marzi A, Engelman F, Feldmann F, Haberthur K, Shupert WL, Brining D, Scott DP, Geisbert TW, Kawaoka Y, Katze MG, Feldmann H, Messaoudi I. 2013. Antibodies are necessary for rVSV/ZEBOV-GP-mediated protection against lethal Ebola virus challenge in nonhuman primates. *Proc Natl Acad Sci U S A* 110:1893–1898. <https://doi.org/10.1073/pnas.1209591110>.
 45. Wec AZ, Nyakatura EK, Herbert AS, Howell KA, Holtsberg FW, Bakken RR, Mittler E, Christin JR, Shulenin S, Jangra RK, Bharrhan S, Kuehne AI, Bornholdt ZA, Flyak AI, Sapphire EO, Crowe JE, Aman MJ, Dye JM, Lai JR, Chandran K. 2016. A “Trojan horse” bispecific-antibody strategy for broad protection against ebolaviruses. *Science* 354:350–354. <https://doi.org/10.1126/science.aag3267>.
 46. Hung T (ed). 1988. Atlas of hemorrhagic fever with renal syndrome. Science Press, Beijing, China.
 47. Hung T, Xia SM, Zhao TX, Zhou JY, Song G, Liao GXH, Ye WW, Chu YL, Hang CS. 1983. Morphological evidence for identifying the viruses of hemorrhagic fever with renal syndrome as candidate members of the bunyaviridae family. *Arch Virol* 78:137–144. <https://doi.org/10.1007/BF01310869>.
 48. Shi X, Elliott RM. 2002. Golgi localization of Hantaan virus glycoproteins requires coexpression of G1 and G2. *Virology* 300:31–38. <https://doi.org/10.1006/viro.2002.1414>.
 49. Ogino M, Yoshimatsu K, Ebihara H, Araki K, Lee B-H, Okumura M, Arikawa J. 2004. Cell fusion activities of Hantaan virus envelope glycoproteins. *J Virol* 78:10776–10782. <https://doi.org/10.1128/JVI.78.19.10776-10782.2004>.
 50. Pettersson RF, Melin L. 1996. Synthesis, assembly, and intracellular transport of bunyaviridae membrane proteins, p 159–188. In Elliott RM (ed), *The Bunyaviridae*. Springer US, Boston, MA.
 51. Shi X, Kohl A, Li P, Elliott RM. 2007. Role of the cytoplasmic tail domains of Bunyamwera orthobunyavirus glycoproteins Gn and Gc in virus assembly and morphogenesis. *J Virol* 81:10151–10160. <https://doi.org/10.1128/JVI.00573-07>.
 52. Overby AK, Popov VL, Pettersson RF, Neve EPA. 2007. The cytoplasmic tails of Uukuniemi virus (Bunyaviridae) G(N) and G(C) glycoproteins are important for intracellular targeting and the budding of virus-like particles. *J Virol* 81:11381–11391. <https://doi.org/10.1128/JVI.00767-07>.
 53. Spiropoulou CF, Goldsmith CS, Shoemaker TR, Peters CJ, Compans RW. 2003. Sin Nombre virus glycoprotein trafficking. *Virology* 308:48–63. [https://doi.org/10.1016/S0042-6822\(02\)00092-2](https://doi.org/10.1016/S0042-6822(02)00092-2).
 54. Spiropoulou CF. 2001. Hantavirus maturation. *Curr Top Microbiol Immunol* 256:33–46.
 55. Ravkov EV, Nichol ST, Compans RW. 1997. Polarized entry and release in epithelial cells of Black Creek Canal virus, a New World hantavirus. *J Virol* 71:1147–1154.
 56. Goldsmith CS, Elliott LH, Peters CJ, Zaki SR. 1995. Ultrastructural characteristics of Sin Nombre virus, causative agent of hantavirus pulmonary syndrome. *Arch Virol* 140:2107–2122. <https://doi.org/10.1007/BF01323234>.
 57. Deyde VM, Rizvanov AA, Chase J, Ottesson EW, St Jeor SC. 2005. Interactions and trafficking of Andes and Sin Nombre Hantavirus glycoproteins G1 and G2. *Virology* 331:307–315. <https://doi.org/10.1016/j.virol.2004.11.003>.
 58. Hepojoki J, Strandin T, Wang H, Vapalahti O, Vaeheri A, Lankinen H. 2010. Cytoplasmic tails of hantavirus glycoproteins interact with the nucleocapsid protein. *J Gen Virol* 91:2341–2350. <https://doi.org/10.1099/vir.0.021006-0>.
 59. Strandin T, Hepojoki J, Wang H, Vaeheri A, Lankinen H. 2011. The cytoplasmic tail of hantavirus Gn glycoprotein interacts with RNA. *Virology* 418:12–20. <https://doi.org/10.1016/j.virol.2011.06.030>.
 60. Andersson AM, Melin L, Bean A, Pettersson RF. 1997. A retention signal necessary and sufficient for Golgi localization maps to the cytoplasmic tail of a Bunyaviridae (Uukuniemi virus) membrane glycoprotein. *J Virol* 71:4717–4727.
 61. Andersson AM, Pettersson RF. 1998. Targeting of a short peptide derived from the cytoplasmic tail of the G1 membrane glycoprotein of Uukuniemi virus (Bunyaviridae) to the Golgi complex. *J Virol* 72:9585–9596.
 62. Gerrard SR, Li L, Barrett AD, Nichol ST. 2004. Ngari virus is a Bunyamwera virus reassortant that can be associated with large outbreaks of hemorrhagic fever in Africa. *J Virol* 78:8922–8926. <https://doi.org/10.1128/JVI.78.16.8922-8926.2004>.
 63. Matsuoka Y, Chen SY, Compans RW. 1994. A signal for Golgi retention in the bunyavirus G1 glycoprotein. *J Biol Chem* 269:22565–22573.
 64. Matsuoka Y, Chen SY, Holland CE, Compans RW. 1996. Molecular determinants of Golgi retention in the Punta Toro virus G1 protein. *Arch Biochem Biophys* 336:184–189. <https://doi.org/10.1006/abbi.1996.0547>.
 65. Shi X, Lappin DF, Elliott RM. 2004. Mapping the Golgi targeting and retention signal of Bunyamwera virus glycoproteins. *J Virol* 78: 10793–10802. <https://doi.org/10.1128/JVI.78.19.10793-10802.2004>.
 66. Guardado-Calvo P, Rey FA. 2017. The envelope proteins of the Bunyavirales. *Adv Virus Res* 98:83–118. <https://doi.org/10.1016/bs.avir.2017.02.002>.
 67. Barriga GP, Villalón-Letelier F, Márquez CL, Bignon EA, Acuña R, Ross BH, Monasterio O, Mardones GA, Vidal SE, Tischler ND. 2016. Inhibition of the

- hantavirus fusion process by predicted domain III and stem peptides from glycoprotein Gc. *PLoS Negl Trop Dis* 10:e0004799. <https://doi.org/10.1371/journal.pntd.0004799>.
68. Guardado-Calvo P, Bignon EA, Stettner E, Jeffers SA, Pérez-Vargas J, Pehau-Arnaudet G, Tortorici MA, Jestin J-L, England P, Tischler ND, Rey FA. 2016. Mechanistic insight into Bunyavirus-induced membrane fusion from structure-function analyses of the hantavirus envelope glycoprotein Gc. *PLoS Pathog* 12:e1005813. <https://doi.org/10.1371/journal.ppat.1005813>.
69. Willensky S, Bar-Rogovsky H, Bignon EA, Tischler ND, Modis Y, Dessau M. 2016. Crystal structure of glycoprotein C from a hantavirus in the post-fusion conformation. *PLoS Pathog* 12:e1005948. <https://doi.org/10.1371/journal.ppat.1005948>.
70. Robison CS, Whitt MA. 2000. The membrane-proximal stem region of vesicular stomatitis virus G protein confers efficient virus assembly. *J Virol* 74:2239–2246. <https://doi.org/10.1128/JVI.74.5.2239-2246.2000>.
71. Mazor Y, Barnea I, Keydar I, Benhar I. 2007. Antibody internalization studied using a novel IgG binding toxin fusion. *J Immunol Methods* 321:41–59. <https://doi.org/10.1016/j.jim.2007.01.008>.
72. Whelan SP, Ball LA, Barr JN, Wertz GT. 1995. Efficient recovery of infectious vesicular stomatitis virus entirely from cDNA clones. *Proc Natl Acad Sci U S A* 92:8388–8392. <https://doi.org/10.1073/pnas.92.18.8388>.
73. Crooks GE, Hon G, Chandonia JM, Brenner SE. 2004. WebLogo: a sequence logo generator. *Genome Res* 14:1188–1190. <https://doi.org/10.1101/gr.849004>.